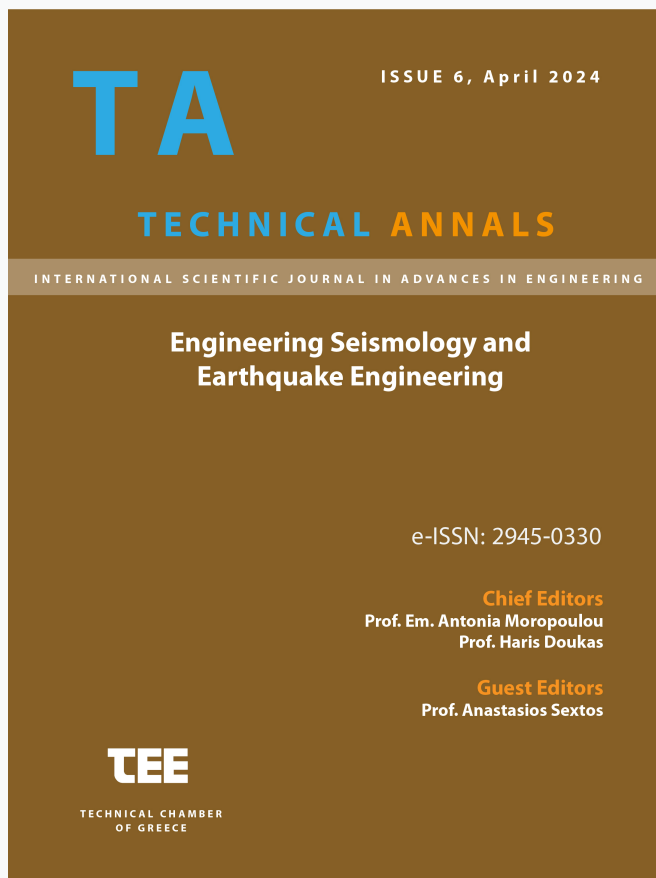


## Technical Annals

Vol 1, No 6 (2024)

Technical Annals



### Seismic risk assessment of buildings and infrastructures using Artificial Neural Networks: Empirical prediction equations

*Konstantinos Morfidis, Dimitrios Sotiriadis, Sotiria Stefanidou, Olga Markogiannaki, Anna Karatzetzou, Basil Margaris*

doi: [10.12681/ta.36895](https://doi.org/10.12681/ta.36895)

Copyright © 2024, Konstantinos Morfidis, Dimitrios Sotiriadis, Sotiria Stefanidou, Olga Markogiannaki, Anna Karatzetzou, Basil Margaris



This work is licensed under a [Creative Commons Attribution-NonCommercial-ShareAlike 4.0](https://creativecommons.org/licenses/by-nc-sa/4.0/).

### To cite this article:

Morfidis, K., Sotiriadis, D., Stefanidou, S., Markogiannaki, O., Karatzetzou, A., & Margaris, B. (2024). Seismic risk assessment of buildings and infrastructures using Artificial Neural Networks: Empirical prediction equations. *Technical Annals*, 1(6). <https://doi.org/10.12681/ta.36895>

# Seismic risk assessment of buildings and infrastructures using Artificial Neural Networks: Empirical prediction equations

Morfidis Konstantinos<sup>1</sup>, Sotiriadis Dimitrios<sup>2</sup>, Stefanidou Sotiria<sup>3</sup>, Markogiannaki Olga<sup>3</sup>, Karatzetzou Anna<sup>4</sup>, Margaris Basil<sup>1</sup>

<sup>1</sup>ITSAK,<sup>2</sup>Democritus University of Thrace,<sup>3</sup>REDI Engineering Solutions PC,

<sup>4</sup>Aristotle University of Thessaloniki

konmorf@gmail.com, dsotiria@civil.duth.gr,  
sotiria.stefanidou@gmail.com, markogiannaki.olga@gmail.com,  
akaratzze@civil.auth.gr, margaris@itsak.gr

**Abstract.** The reliable assessment of the seismic risk, at urban, regional and national level, is extremely important for the government and society and contributes to the proper management of the pre-seismic crisis (interventions, strengthening of buildings and infrastructures), during the earthquake and post-earthquake. The seismic risk assessment involves many difficulties and uncertainties, as it depends on the successful implementation of several individual steps, starting with the identification of the elements at risk, continuing with the assessment of seismic risk and vulnerability and finishing with the estimation of the risk and losses of all types. In all the above methodological frameworks, the use of Artificial Neural Networks (ANNs) is proposed in the literature. Artificial Intelligence (AI)-based methodologies aim to improve the computational efficiency of simulations, by increasing the accuracy and reducing the computational cost. In this paper, a methodology using ANNs at the seismic hazard level is suggested to propose strong motion prediction equations (GMPE) derived from ANN training, by developing a methodological framework and a computational tool that enables continuous training and learning depending on the strong motion data that are fed to it. The proposed equations are compared with models in the literature to verify the reliability of their applicability.

**Keywords:** Seismic risk assessment, seismic hazard, artificial neural networks, ground motion prediction equations, seismic strong motion

## 1 Introduction

The methodologies for the assessment of seismic risk of buildings and infrastructures are a significant tool for the evaluation of the exposure, the prioritization of interventions and the development of a comprehensive upgrade plan. In this context, various methodologies have been developed over the last decades for the determination of the assessed exposure, seismic hazard and seismic fragility, which are the individual steps for the assessment of seismic risk. At the same time, in several cases, computational

tools have been developed which integrate the individual methodologies, but the computational cost and time required for the analysis and calculation of risk remain significant. For this purpose, methodologies have been developed, and utilized in the individual steps of seismic risk determination, that utilize ANNs for their direct and reliable determination. In particular, ANNs have been used to determine seismic vulnerability (Xie et al., 2020, Stefanidou et al., 2021), and very recently they have been proposed for seismic risk assessment (Ji et al., 2021). Additionally, the use of ANNs for seismic risk assessment can be applied to the prediction of seismic losses in areas with high seismicity (e.g. Leousis and Pnevmatikos, 2018, Pnevmatikos et al., 2020).

This paper presents a first step of a holistic seismic risk assessment methodology to be developed. The proposed methodology will be an integrated, versatile and easy-to-use methodology for assessing the vulnerability and seismic risk of buildings and infrastructures, fully adapted to the Greek data. It will be an important tool in the hands of the relevant authorities, contributing to the identification and recommendation of cost-effective lines of intervention and guidelines for addressing the problem pre-seismically and leading to the development of a common strategic plan to improve the resilience of buildings and infrastructures. More specifically, one of the most important steps of any seismic risk assessment methodology will be presented here, which is the assessment of the seismic hazard model. Ground motion predictive equations (GMPEs) derived from ANN training will be proposed, developing a methodological framework and a computational tool that enables continuous training and learning according to the strong motion (SM) data it is supplied with, and a comparison with models proposed in the literature will be presented to verify its applicability.

## 2 The method

The proposed methodology, part of which will be presented in the present paper, is illustrated in the form of a flowchart in Fig. 1.

The first step is the selection of the building stock and infrastructure to be studied and their visualization in a GIS application. The second step is the assessment of the seismic risk, which is the subject of the present study. The seismic hazard assessment of the study area is a necessary component in the seismic risk assessment. For this reason, a seismic hazard analysis is required. Rather than using a deterministic model for the worst earthquake that may affect the region of interest, probabilistic hazard analysis (PSHA) adopts a probability-based framework that considers all earthquake events that may occur in that region (Baker, 2008). PSHA begins by identifying potential earthquake sources and characterizing the distribution of earthquake magnitudes and distance from the source. Then the GMPEs are derived which give the earthquake intensity measure (IM) as a function of the earthquake source, path and local site conditions. One of the key steps of PSHA is therefore the calculation of appropriate GMPEs. There are several methodologies to derive these relationships and in some of them, the use of ANN is suggested (Ji et al., 2021).

The next step is the assessment of the seismic vulnerability through the vulnerability curves and the visualization of the vulnerability in a GIS platform. Numerical

simulations based on the finite element method (FEM) are widely used to derive appropriate vulnerability curves. For reliable vulnerability assessment, a large number of numerical analyses are required, thus increasing the computational cost. One way to reduce this computational cost is the construction of meta-models, which can replace time-consuming FEM models. Meta-models, such as artificial neural networks (ANNs), represent a set of sophisticated statistical algorithms that capture input-output relations of physical models and make predictions according to these relations.

Finally, with the synthesis of all the above steps, the seismic risk for the study area and the exposed elements under study can be derived.

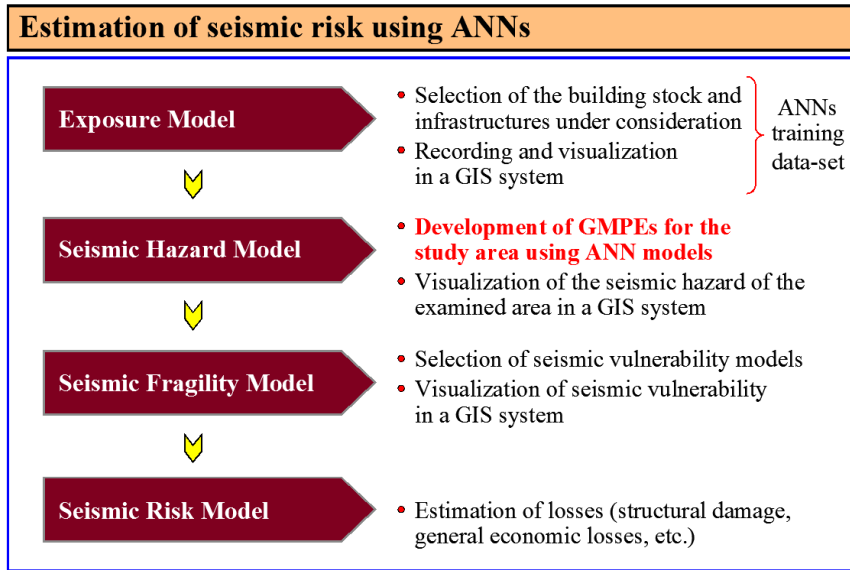


Fig. 1. Methodological framework for seismic risk assessment using ANNs

### 3 Development of equations by means of ANNs

In this section, the process of formulating the equations developed by applying ANNs will be briefly presented. These equations concern the correlation of PGA and PGV with the parameters of earthquake magnitude ( $M_w$ ), its Focal Mechanism (FM), the shear wave velocity  $V_{s30}$  at the site of recording, and the distance of the recording site from the projection of the rupture point on the surface ( $R_{JB}$ ). The general form of the equations to be developed is:

$$\ln(\text{PGA})=f_{\text{PGA}}[M_w, \text{FM}, \ln(V_{s30}), \ln(R_{JB})] \text{ and } \ln(\text{PGV})=f_{\text{PGV}}[M_w, \text{FM}, \ln(V_{s30}), \ln(R_{JB})] \quad (1)$$

The equations were developed by applying Multilayered Feedforward Perceptron Neural Networks (MFPNN) (Haykin, 2009) which have the general form of Fig. 2. The application of MFPNNs and in particular those with a hidden layer has been proven to

lead to the approximation of unknown functions (Hornik et al., 1989) by training them with appropriate training sample sets (training datasets). The procedure for deriving equations approximating unknown functions via MFPNN is described in detail in the paper of Morfidis and Kostinakis (2019).

As regards the training of the networks, it should be noted that a database consisting of 2492 samples was used. This database has been presented by Margaritis et al. (2021) and is the most up-to-date in terms of SM data for the Greek region. An extensive parametric investigation was performed in order to identify the network configuration that leads to the optimal results. In the first stage, the criteria for the evaluation of the results extracted from the examined networks concerned the correlation factor R (R-factor) and the Mean Square Error (MSE). The parameters investigated are presented in Fig. 2.

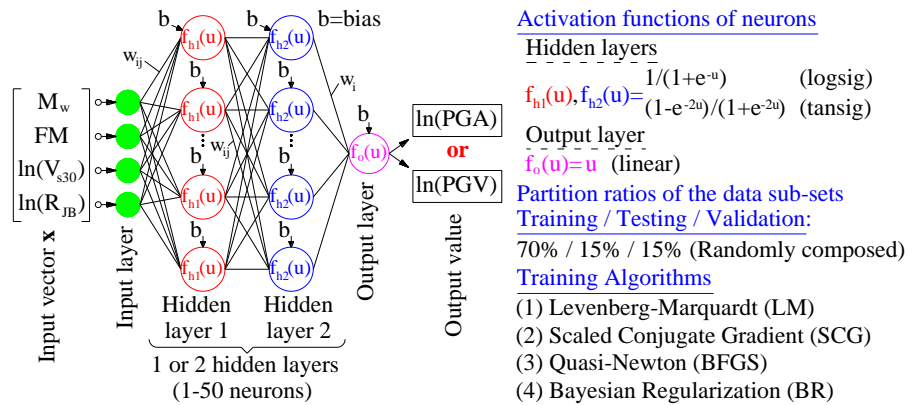


Fig. 2. Configuration and investigated parameters of the networks used

The training procedure applied is the cross-validation method for selecting the optimal model (Diamantaras and Botsis, 2019) which consists of the following 2 stages:

- Randomly dividing the set of training samples  $N$  times into three subsets and training the ANN with the training sub-set (training data sub-set, Fig. 2). In this process, all the ANN configuration parameters, as well as, the training algorithm are examined and finally the parameters that lead to the optimal performance (here based on the selected evaluation parameters R-factor and MSE) for the test sample portion (testing data sub-set, Fig. 2) are selected.
- After determining the parameters that compose the ANNs with optimal performance according to the criteria of the previous step, these networks are re-trained with the whole training dataset without splitting it into sub-sets.

In the context of the present study, the MFPNNs examined were initially classified into three general categories:

- (a) Networks with one hidden layer and with a number of neurons ranging from 1 to 5. These networks were investigated to determine whether they can extract reliable correlation equations of the examined parameters since the small number of neurons leads to the extraction of closed elegant relations.

- (b) In networks with a hidden layer and with a number of neurons ranging from 6 to 30. These networks were investigated to examine how much a larger number of neurons can improve the correlation level.
- (c) In networks with two hidden layers. Although networks with one hidden layer are capable of approximating unknown functions, the performance of networks with two hidden layers was also investigated. The addition of the second hidden layer significantly increases both the complexity and the training time especially when a large number of networks with different configurations are investigated as in the present case. Thus, the aim was to investigate whether this large increase in complexity is also reflected in the increase in performance of the corresponding networks.

The module of machine and deep learning of MATLAB R2022a was used for the development of ANNs and their training process. Table 1 summarizes the results for the optimal configurations of the networks of the three general categories.

**Table 1.** Comparative evaluation of the performance of the examined MFPNNs

| SM Parameter /<br>Evaluation Parameter | 1 Hidden layer                     |                |                                    |                        | 2 Hidden layers                    |  |
|--|------------------------------------|----------------|------------------------------------|------------------------|------------------------------------|--|
|  | Number of neurons $\leq 5$         |                | Number of neurons $> 5$            |                        | Number of neurons 1-50 / layer     |  |
|  | Training Algorithm / Configuration |                | Training Algorithm / Configuration |                        | Training Algorithm / Configuration |  |
| <b>PGA</b><br>(cm/sec <sup>2</sup> )   | <b>maxR</b>                        | BR/log-5 0.934 | BR/tan-13 0.935                    | BR/tan-log/36-24 0.936 |                                    |  |
|  | <b>minMSE</b>                      | BR/log-5 0.524 | BR/log-18 0.518                    | BR/tan-tan/20-8 0.510  |                                    |  |
| <b>PGV</b><br>(cm/sec)                 | <b>maxR</b>                        | BR/log-5 0.921 | BR/log-23 0.922                    | BR/log-log/14-38 0.924 |                                    |  |
|  | <b>minMSE</b>                      | BR/tan-4 0.471 | BR/log-23 0.467                    | BR/tan-log/36-14 0.453 |                                    |  |

The most important conclusion drawn from the study in Table 1 is that adding a large number of neurons and/or a second hidden layer does not substantially improve the values of the R and MSE evaluation parameters. This means that it is possible to select MFPNN models with one hidden layer and number of neurons less than or equal to five. An additional important conclusion is that in all studied cases the BR algorithm led to the most reliable results however with very small differences from the other algorithms considered. Based on the above conclusions it was considered sufficient to focus on network models with a hidden layer. For these models it can be shown (see e.g. Morfidis and Kostinakis, 2019) that the correlation relationship they extract has the form of Eq. 2 and Eq. 3. More specifically:

- (a) In the case where the activation function of the hidden layer neurons is the logsig function (Fig. 2):

$$\ln(\text{PGA}) = \frac{1}{2} \cdot \left\{ \max[\ln(\text{PGA})]_{\text{ds}} - \min[\ln(\text{PGA})]_{\text{ds}} \right\} \cdot \left[ \ln(\text{PGA})^{(\text{norm})} + 1 \right] + \min[\ln(\text{PGA})]_{\text{ds}}$$

$$\left[ \ln(\text{PGA}) \right]^{(\text{norm})} = \sum_{i=1}^{\text{nn}} \left[ \frac{w_i^{(o)}}{1 + e^{-g_i}} \right] + b^{(o)} \quad (2)$$

$$g_i = b_i^{(\text{int})} + w_{i1}^{(\text{int})} \cdot M_w^{(\text{norm})} + w_{i2}^{(\text{int})} \cdot \text{FM}^{(\text{norm})} + w_{i3}^{(\text{int})} \cdot \left[ \ln(V_{S30}) \right]^{(\text{norm})} + w_{i4}^{(\text{int})} \cdot \left[ \ln(R_{JB}) \right]^{(\text{norm})}$$

(b) In the case where the activation function of the hidden layer neurons is the tansig function (Fig. 2) then the only difference with respect to Eq. 2 is the following: Where in Eqs. 2 and 3:

nn is the number of neurons in the hidden layer,  
 $w_{ij}$  is the value of the synaptic weight of the synapse connecting neuron i of the hidden layer to neuron j of the input layer (the values of  $w_{ij}$  comprise a dimensional matrix  $n \times m$  where  $n = \text{nn}$  and  $m = 4 = \text{number of input parameters as given in Fig. 2}$ ),  
 $w_i$  is the value of the synaptic weight of the synapse connecting the hidden layer neuron i to the output neuron (the values of  $w_i$  comprise a vector  $n \times 1$ )  
 $b_i$  is the value of the bias of neuron i (for the neurons in the hidden layer,  $b_i$  comprise a vector  $n \times 1$ , and since the output layer neuron is one,  $b_i$  in this case is a scalar parameter),  
the exponent (o) denotes the output level,  
the exponent (int) denotes the hidden level,  
the exponent (norm) denotes a normalized value, i.e. the value of the input or output parameter after transforming it through the following normalization function:

$$X^{(\text{norm})} = 2 \cdot \left[ \frac{X^{(\text{input})} - \min(X)_{\text{ds}}}{\max(X)_{\text{ds}} - \min(X)_{\text{ds}}} \right] - 1 \quad X = M_w, \text{FM}, \ln(V_{S30}), \ln(R_{JB}) \quad (3)$$

Where in the above function:  
the subscript ds denotes the training sample (data set),  
the exponent (input) indicates that the value X is the value of the parameter to be given as input to the trained network in order for it to extract the prediction for the PGA or PGV,  
the value max refers to the max value of the parameter X in the training sample ds,  
the value min refers to the min value of parameter X in the training sample ds.

Obviously, completely analogous equations to the above apply to the PGV parameter but with different values of the synaptic weights w and biases b as obtained after the training procedures of the respective MFPNNs.

Finally, it should be noted that values of synaptic weights and biases of all optimal trained networks in Table 1 with one hidden layer are available at the following hyper-link ([link](#)).

## 4 Comparison of ANN relations with SM data and other relations

Figs. 3a - 3d show comparisons of PGA estimates from the new ANN based equations, existing GMPEs and strong motion (SM) data for two ranges of seismic magnitudes. Of the existing equations presented, the Boore et al. (2021) equation is the most recent GMPE for the Greece, while the Kotha et al. (2020) and Chiou and Youngs (2014) equations have been shown to be accurate for ground motion estimation in Greece. Regarding PGA, it is observed that the ANN based equations show similar trends with both SM data and existing GMPEs. For earthquakes with magnitudes less than M6.0 and close distances, the BR\_LOG\_5F1 equation gives quite similar values to the equation of Boore et al. (2021), while for distances greater than 30 km the estimates of the former are lower than the latter. The pattern is similar for BR\_TAN\_13F1 equation, while BR\_LOG\_18F1 equation estimates higher values than Boore et al. (2021) in the near field. At long distances, where more data are available, the ANN based equations give similar estimates. The pattern is similar for earthquakes larger than M6.0, with the differences in the near-field between ANN equations and Boore et al. (2021) becoming sharper. In fact, the estimates of BR\_LOG\_18F1 and BR\_TAN\_13F1 equations yield higher estimates than all other equations presented. Regarding PGV, the proposed ANN equations give similar estimates to each other, except for the near-field (<10 km) and earthquakes larger than M6.0. For the same magnitude range, the estimates of the ANN equations are higher than those of Boore et al. (2021) and are close to the estimates of the Chiou and Youngs (2014) model. For smaller magnitude earthquakes, the estimates of the proposed relations are similar to those of Boore et al. (2021). It is notable that the differences between the displayed equations (new and existing) become sharper in regions where there is a lack of data.

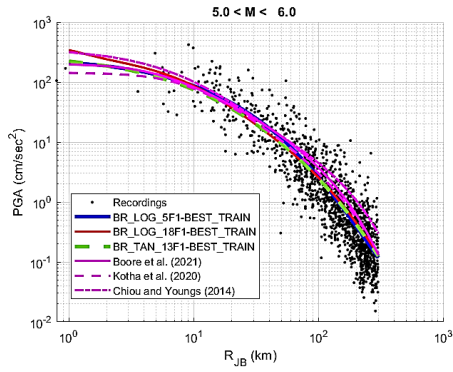


**Fig. 3a.** Comparison between PGA estimation from ANN equations, existing GMPEs and SM data for  $5.0 < M < 6.0$  earthquakes

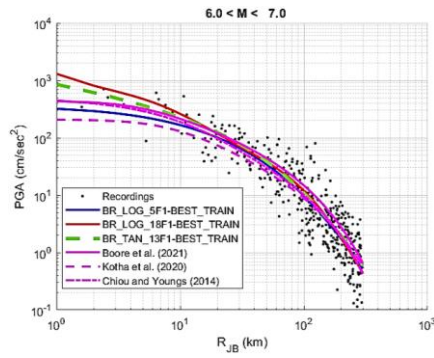


**Fig. 3b.** Comparison between PGA estimation from ANN equations, existing GMPEs and SM data for  $6.0 < M < 7.0$  earthquakes



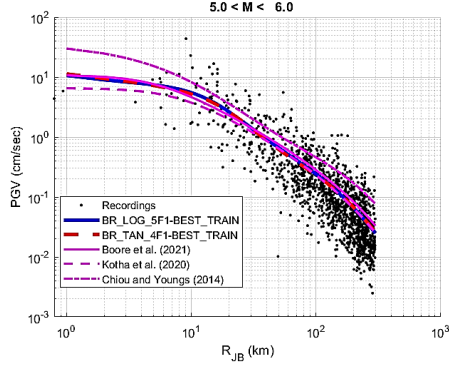


**Fig. 3c.** Comparison between PGV estimation from ANN equations, existing GMPEs and SM data for  $5.0 < M < 6.0$  earthquakes

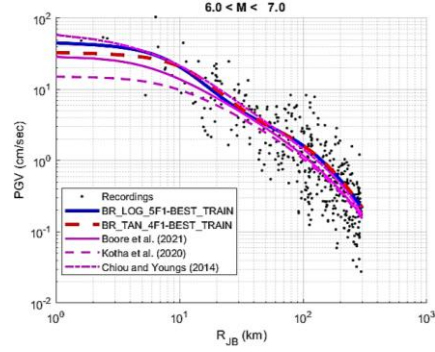


**Fig. 3d.** Comparison between PGV estimation from ANN equations, existing GMPEs and SM data for  $6.0 < M < 7.0$  earthquakes

## 5 Residual analysis

In the context of GMPE development, residuals are defined according to Eq. 4, where  $R$  is the residual, indices  $i$  and  $j$  indicate a seismic event and a location, respectively,  $\ln(Y_{ij})$  is the observed value of the SM, and  $\mu_{\ln Y}$  is the log mean estimate of the SM from a model.

$$R_{ij} = \ln(Y_{ij}) - \mu_{\ln Y}(M^i, R_{JB}^{ij}, V_{S30}^j, mech^i) \quad (4)$$

The mixed-effects analysis (Abrahamson and Youngs, 1992) is applied to the residuals in order to separate them into between-event residuals and within-event residuals, according to Eq. 5. In Eq. 5,  $B$  is the total bias,  $\eta_i$  and  $\varepsilon_{ij}$  are the between- and within-event residuals, respectively. These errors are assumed to be normally distributed with zero mean and standard deviation  $\tau$  and  $\phi$ , respectively. The overall standard deviation,  $\sigma$ , is given by Eq. 6.

$$R_{ij} = B + \eta_i + \varepsilon_{ij} \quad (5)$$

$$\sigma = \sqrt{\tau^2 + \phi^2} \quad (6)$$

Residual analysis, between mean estimates and SM data, was conducted for the proposed ANN equations and the equation of Boore et al. (2021). The results are presented in Figs. 4 and 5 for the PGA and PGV parameters, respectively. It is observed that the use of ANNs smooths out the small deviation and trend observed in the error  $\eta_i$  with respect to the earthquake magnitude for the Boore et al. (2021) model for both PGA and PGV. Regarding the error  $\varepsilon_{ij}$  with respect to the  $R_{JB}$  distance, the pattern is similar between ANN and Boore et al. (2021) models, while, a slight improvement in the error  $\varepsilon$  with respect to the  $V_{S30}$  velocity is observed from the ANN equations.

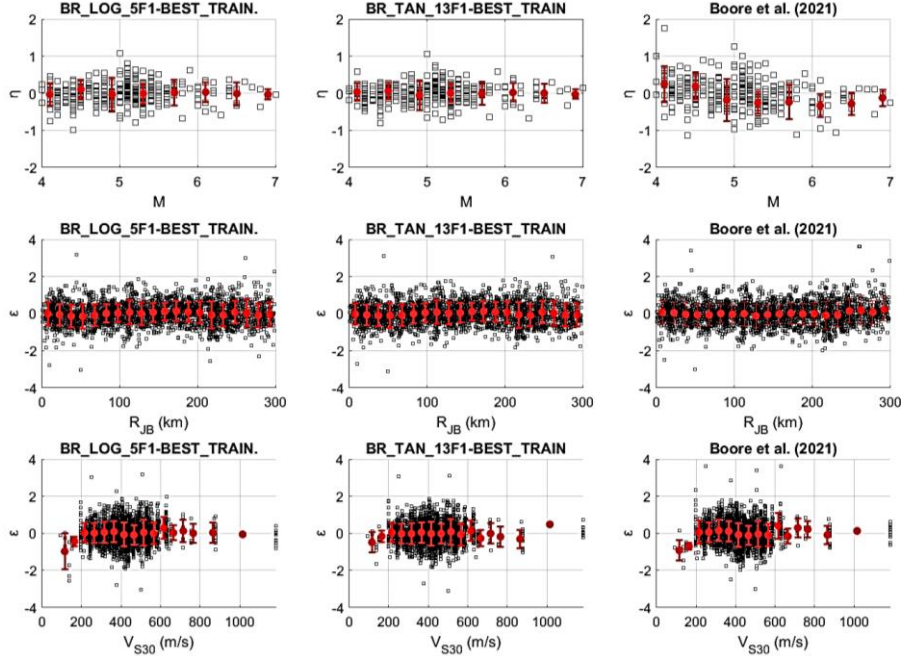


**Fig. 4.** Residual analysis between ( $\eta$ ) and within ( $\epsilon$ ) seismic event for the proposed ANN and GMPE equations of Boore et al. (2021) for PGA

In Fig. 6, the values of the standard deviation of the between-event ( $\tau$ ) and within-event ( $\epsilon$ ) residuals, as well as, the total standard deviation ( $\sigma$ ), for the ANN models, are presented with respect to the earthquake magnitude. These values are compared with the uncertainty model proposed by Boore et al. (2021). For the PGA (Fig. 6a), it is observed that the BR\_TAN13F1 model has smaller standard deviations than the BR\_LOG5F1 model. Also, the standard deviations of the two models are comparable to the values of Boore et al. (2021), however they seem relatively stable for all earthquake magnitudes, except for large magnitudes where there are not enough data. The pattern is similar for PGV (Fig. 6b), except that the ANN models show similar values of standard deviations. Table 2 shows the selected fixed standard deviation values for the ANN models, as selected based on Fig. 6, compared to the standard deviations of Boore et al. (2021). In general, similar standard deviations are observed between ANN and Boore et al. (2021), with ANN giving slightly smaller overall standard deviation values.

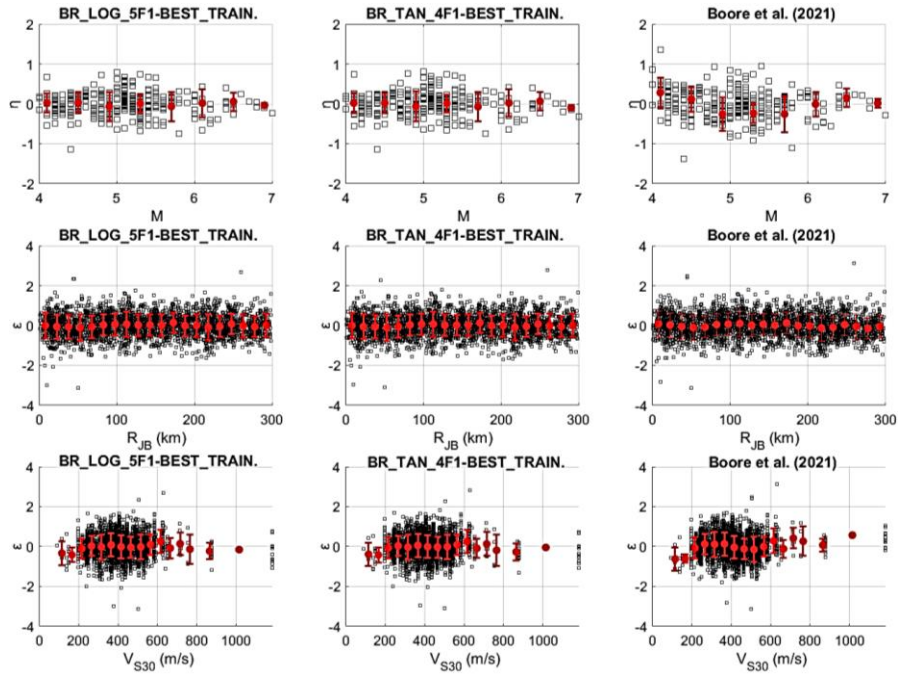


**Fig. 5.** Residual analysis between ( $\eta$ ) and within ( $\epsilon$ ) seismic event for the proposed ANN and GMPE equations of Boore et al. (2021) for PGV

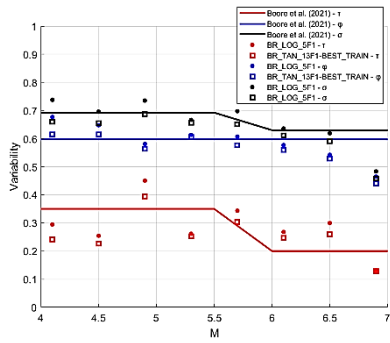


**Fig. 6a.** Uncertainty models of ANN equations compared to the GMPE of Boore et al. (2021), for PGA

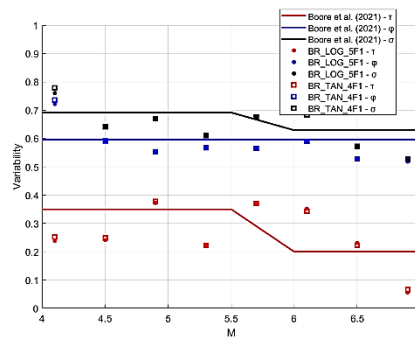


**Fig. 6b.** Uncertainty models of ANN equations compared to the GMPE of Boore et al. (2021), for PGV

**Table 2.** Selected standard deviation values for the ANN models

| GMPE                       | PGA                |        |          | PGV                |        |          |
|----------------------------|--------------------|--------|----------|--------------------|--------|----------|
|                            | $\tau$             | $\phi$ | $\sigma$ | $\tau$             | $\phi$ | $\sigma$ |
| <b>BR_LOG5F1</b>           | 0.305              | 0.601  | 0.674    | 0.278              | 0.569  | 0.633    |
| <b>BR_LOG13F1</b>          | 0.279              | 0.586  | 0.649    | -                  | -      | -        |
| <b>BR_TAN4F1</b>           | -                  | -      | -        | 0.279              | 0.568  | 0.633    |
| <b>Boore et al. (2021)</b> | M $\leq$ 5.5: 0.35 | 0.597  | 0.692    | M $\leq$ 5.5: 0.35 | 0.596  | 0.691    |
|                            | M $\geq$ 6.0: 0.20 |        | 0.630    | M $\geq$ 6.0: 0.20 |        | 0.629    |

## 6 Conclusions

In the present paper, a GMPE for Greece for seismic risk assessment, which has been derived from ANN training, is proposed and compared with models proposed in the literature to verify the reliability of its applicability. Based on the results presented in the previous sections, it is evident that the proposed relation can be used to estimate both PGA and PGV accurately, as the observed error is within reasonable limits. Also, similar standard deviations are observed between ANN and the equations in the literature with ANN giving slightly smaller overall standard deviation values.

## References

1. Xie, Y, Ebad Sichani, M., Padgett, J. E. & DesRoches, R. (2020) The promise of implementing machine learning in earthquake engineering: A state-of-the-art review. *Earthquake Spectra*, 36(4), 1769–180.
2. Stefanidou S.P., Papanikolaou V.K., Paraskevopoulos E.A., Kappos, A.J., (2021) Machine learning techniques for the estimation of limit state thresholds and bridge-specific fragility analysis of RC bridges. 8th ECCOMAS Thematic Conference on Computational Methods in Structural Dynamics and Earthquake Engineering, COMPDYN 2021, Athens, 27-30 June
3. Ji, D., C. Li, C. Zhai, Y. Dong, E. I. Katsanos, and W. Wang (2021). Prediction of Ground-Motion Parameters for the NGA-West2 Database Using Refined Second-Order Deep Neural Networks, *Bull. Seismol. Soc. Am.* 111, 3278–3296, doi: 10.1785/0120200388
4. Leousis D., Pnevmatikos N., (2018) Earthquake losses assessment in the municipality of Kifissia (Athens – Greece) using the Earthquake Loss Estimation Routine (ELER). *International Journal of Earthquake Engineering and Hazard Mitigation (IREHM)*, 6(1), 11-20.
5. Pnevmatikos N, Konstandakopoulou F, Koumoutsos N (2020) Seismic vulnerability assessment and loss estimation in Cephalonia and Ithaca islands, Greece, due to earthquake events: a case study. *Soil Dyn Earthq Eng* 136:106252. <https://doi.org/10.1016/j.soildyn.2020.106252>
6. Baker, J. W. & Jayaram, N. (2008). Correlation of spectral acceleration values from NGA ground motion models. *Earthquake Spectra*, 24(1), 299–317

7. Haykin S. *Neural networks and learning machines*. 3rd ed. Prentice Hall; 2009
8. Hornik K, Stinchcombe M, White H. Multilayer Feedforward Networks are Universal Approximators. *Neural Networks* 1989;2(5):359-366
9. Konstantinos E. Morfidis and Konstantinos G. Kostinakis. Use of artificial neural networks in the R/C buildings' seismic vulnerability assessment: the practical point of view. In: *Proceedings of 7th Conference in Computational Methods in Structural Dynamics and Earthquake Engineering (COMPDYN2019)*, Crete island, Greece, 24-26 June 2019 (Paper Number: C19299)
10. Margaritis, B., E. Scordilis, J.P. Stewart, D.M. Boore, N. Theodoulidis, I. Kalogeras, N. Melis, A. Skarlatoudis, N. Klimis, and E.Seyhan (2021). Hellenic Strong-Motion Database with Uniformly Assigned Source and Site Metadata for period of 1972-2015, *Seismological Research Letters*, Vol. 92, No. 3, pp 2065– 2080
11. K. Diamantaras and D. Botsis, *Machine Learning*, "Klidarithmos" Publications, Athens 2019 (In Greek).
12. Boore, D. M., J. P. Stewart, A. A. Skarlatoudis, E. Seyhan, B. Margaritis, N. Theodoulidis, E. Scordilis, I. Kalogeras, N. Klimis, and N. S. Melis. A Ground-Motion Prediction Model for Shallow Crustal Earthquakes in Greece, *Bulletin of the Seismological Society of America* 2021; 111(2): 857–874
13. Kotha S. R., Weatherhil G., Bindi D., Cotton F. A regionally-adaptable ground motion model for shallow crustal earthquakes in Europe, *Bulletin of Earthquake Engineering* 2020; 18: 4091 – 4125
14. Chiou B. S.-J., Youngs R. R. Update of the Chiou and Youngs NGA model for the average horizontal component of peak ground motion and response spectra, *Earthquake Spectra* 2014; 30: 1117 – 1153
15. Abrahamson N., Youngs R. A stable algorithm for regression analyses using the random effects model, *Bulletin of the Seismological Society of America* 1992; 82: 505 – 510